The Journal of Experimental Biology **198**, 1575–1587 (1995)
Printed in Great Britain © The Company of Biologists Limited 1995

RED MUSCLE MOTOR PATTERNS DURING STEADY SWIMMING IN LARGEMOUTH BASS: EFFECTS OF SPEED AND CORRELATIONS WITH AXIAL KINEMATICS

BRUCE C. JAYNE[1] AND GEORGE V. LAUDER[2]

[1]*Department of Biological Sciences, University of Cincinnati, Cincinnati, OH 45221-0006, USA* and
[2]*Department of Ecology and Evolutionary Biology, University of California, Irvine, CA 92717, USA*

Accepted 9 March 1995

Summary

We analyzed midline kinematics and obtained electromyograms (EMGs) from the superficial red muscle at seven longitudinal positions in four largemouth bass swimming steadily at standardized speeds of 0.7, 1.2, 1.6, 2.0 and 2.4 lengths s^{-1}. Analysis of variance was used to test for significant variation attributable to both speed and longitudinal position. EMGs propagated posteriorly were unilateral and alternated between the left and right sides. Despite the propagation of EMGs, all the red muscle along an entire side of the fish was simultaneously active for as much as one-quarter of the locomotor cycle. When expressed as a proportion of the locomotor cycle, EMG durations at a given site did not vary significantly with speed but did vary longitudinally, ranging from values of 0.45 cycles anteriorly to 0.35 cycles posteriorly. The amplitudes of lateral displacement and bending depended on longitudinal position and also increased by a maximum of approximately 50 % with increased swimming speed, whereas for all longitudinal positions the intensity of EMGs increased approximately fourfold with increased swimming speed. Electrical activity of red muscle did not correspond simply to the time of muscle shortening. Instead, the timing of EMG onset and offset relative to both lateral bending and displacement changed significantly with both longitudinal position and increased speed, such that the phase shifts between the EMGs and kinematic values were generally greatest for posterior sites at the fastest speeds. At a single longitudinal position, the phase shift between the EMG and maximal lateral bending could change by more than one-tenth of a cycle from the slowest to the fastest swimming speed. Phase lags per body segment of EMG onset and EMG offset did not vary significantly with either swimming speed or longitudinal position. EMG offset was propagated posteriorly faster than EMG onset, and both EMG onset and EMG offset were generally propagated faster than both lateral bending and displacement. Largemouth bass have a similar number of vertebrae to carp, and these two species also have a very similar pattern of muscle activation that differs substantially from that of the trout, which has nearly twice as many vertebrae.

Key words: locomotion, fish, largemouth bass, *Micropterus salmoides*, muscle, electromyography, swimming.

Introduction

The rhythmic axial undulations of fishes swimming at steady speeds have been an exemplary experimental system for gaining insights into the neural control and muscle function that are responsible for locomotor movements. For example, fictive preparations of such diverse species as sharks (Bone, 1966), lamprey (Wallén and Williams, 1984) and goldfish (Fetcho and Svoboda, 1993) have shown that circuitry within the spinal cord is sufficient to generate a pattern of alternating unilateral activation of muscle that is posteriorly propagated and is characteristic of *in vivo* observations of muscle activity. In addition, recent application of the work loop method for studying *in vitro* preparations of fish muscle have yielded considerable insights into power output and how it is affected by differences in swimming speed and longitudinal location within the body of a fish (Altringham and Johnston, 1990; Rome and Swank, 1992; Rome *et al.* 1993; Johnson *et al.* 1994). Furthermore, the spatial segregation of different fiber types in the axial muscles of fish has facilitated these *in vitro* studies of muscle physiology as well as *in vivo* observations of muscle recruitment that are associated with speed (Bone *et al.* 1978; Johnston and Moon, 1980; Rome *et al.* 1985; Jayne and Lauder, 1994*a*).

Despite a large literature on the kinematics and muscle activity involved in the undulatory swimming of vertebrates, much remains to be learned about the interrelationships between morphological variation and the coordination of muscle activity. In contrast to the relatively simple posterior propagation of motor output exemplified by fictive

preparations, the propagation of swimming movements of intact organisms appears likely to be a complex result of motor output, the passive and active mechanical properties of the organism and the resistive forces imposed by the environment (Blight, 1977; Jayne and Lauder, 1993; Long *et al.* 1994). The best-studied fish taxa such as lamprey, eel, trout and carp (Grillner and Kashin, 1976; Williams *et al.* 1989; van Leeuwen *et al.* 1990) include so much phylogenetic and morphological diversity that it is difficult to interpret the consequences of any one particular morphological difference. For example, compared with many subcarangiform swimmers, eels and lampreys have both a more elongate external shape and greater numbers of vertebrae (Scott and Crossman, 1973); therefore, external shape differences confound understanding the effects of vertebral number and *vice versa*.

To isolate the effects of external body shape on the relationship between muscle activity and undulatory swimming movements, we have been quantifying morphology and conducting a series of experiments on two closely related subcarangiform swimmers, the largemouth bass *Micropterus salmoides* and the bluegill sunfish *Lepomis macrochirus* (Jayne and Lauder, 1993, 1994*a*,*b*, 1995*a*,*b*). Both of these species belong to a well-defined monophyletic group of perciform teleost fishes (Lauder and Liem, 1983; Mabee, 1993) that has minimal variation in the numbers of vertebrae (Scott and Crossman, 1973), despite the fact that the bass conforms to a generalized fusiform shape (Webb, 1994) whereas the bluegill has a more specialized deep-bodied shape.

Because much of the previous electromyographic research with the subcarangiform swimming of fishes has been motivated primarily by interest in fiber type recruitment (Hudson, 1973; Bone *et al.* 1978; Johnston and Moon, 1980; Rome *et al.* 1985), electromyograms (EMGs) have generally been obtained for few (three or fewer) longitudinal locations, and simultaneous kinematic information has often been sparse (for notable exceptions, see Williams *et al.* 1989; van Leeuwen *et al.* 1990). Consequently, the longitudinal extent of muscle activation, the relationship between EMGs and movement, and the effects of longitudinal position on this relationship are still not well understood for most subcarangiform swimmers. Kinematic studies have commonly documented the effects of speed on the amplitude of lateral displacement, but data on the amplitude of lateral bending are less abundant. Because the strain of the axial musculature is proportional to lateral bending, this is a critical kinematic variable to quantify in order to understand *in vivo* muscle function (Rome *et al.* 1988). Thus, even for a single species of fish, it is presently uncommon to have integrated information on the muscle activity associated with both lateral displacement and bending at several longitudinal locations and on the effects of speed on these quantities. We studied the steady swimming of largemouth bass specifically to obtain such an integrated understanding of muscle activity and movement.

The goal of the present study is to analyze red muscle activity and axial kinematics during steady swimming of the largemouth bass, specifically with the aims of (1) determining muscle activity from a large number of longitudinal locations to facilitate inferring the whole-body pattern of muscle activation, (2) quantifying the amplitude and timing of both lateral displacement and bending, and relating these to the timing of muscle activity, and (3) determining the effect of locomotor speed on the interrelationships between kinematics and muscle activity.

Materials and methods

Experimental subjects and protocol

We obtained specimens of largemouth bass, *Micropterus salmoides* (Lacepède), from ponds in southern and central California. The bass were fed a maintenance diet of earthworms and goldfish and were held in captivity before experiments for less than 3 months. All fish were maintained individually in 40 or 80 l tanks at a temperature of 20±2 °C, which averaged the same value as the water temperature that was used during experiments (20±0.5 °C).

After standardizing methods during preliminary experiments with three individuals, we performed experiments with seven additional individuals from which the data were analyzed. Four of these seven individuals were chosen for complete statistical analysis with the goal of obtaining a maximally balanced statistical design for the analyses of variance (described below). Individual fish not used for the complete statistical analysis had missing data due either to electrodes being pulled out during recording sessions or to subsequent determination that the electrode tips were not in the superficial red muscle fibers.

For the four individuals analyzed, mean values (and ranges) of mass, standard length and total length (L) were 88 g (77–99 g), 16.7 cm (15.8–17.5 cm) and 19.8 cm (18.9–20.4 cm), respectively. Mean tail span approximated 5.1 cm. The numbers of precaudal vertebrae ranged from 14 to 16, and the numbers of vertebrae between the trunk and hypurals ranged from 15 to 16.

After implanting electrodes (see below), we placed the fish into the flow tank and allowed them to recover from anesthesia for 2–3 h before we elicited swimming at steady speeds of 0.7, 1.2, 1.6, 2.0 and 2.4 $L\,s^{-1}$. The working section of the calibrated flow tank was 18 cm×18 cm×46 cm, with the long dimension being parallel to the flow direction. As in previous experiments with steady swimming (Jayne and Lauder, 1995*a*), we only analyzed results from trials where the variation in swimming speed among successive tail beats was less than 5 %. Fish commonly swam nearly in the center of the working section of the flow tank, and we only used trials for which the fish were at least 4 cm away from any wall of the tank and the surface of the water. The gap span ratio of the swimming fish (Webb, 1993) approximated 2.4 when fish were centered and 1.5 for sequences in which fish were closest to a wall of the flow tank. At the conclusion of each experiment, fish were killed with an overdose of anesthetic and fixed in formalin to allow *post-mortem* dissections and X-ray photograph.

Kinematics

Video tapes (synchronized with electromyographic recordings) were obtained simultaneously for both a lateral view and a back-lit ventral view (Jayne and Lauder, 1995*a*) of the swimming fish using a NAC HSV-400 high-speed video system operating at a rate of 200 images s^{-1}. The lateral view was used primarily to ensure that the vertical position of the fish was approximately midway between the bottom of the tank and the surface of the water.

For each swimming speed, video images were digitized at equally spaced time intervals approximating 1/20 of the tail-beat cycle duration for a total time interval slightly greater than four cycles at each speed for each individual. Ventral-view images were analyzed by digitizing 25–30 points along each side of the fish using custom-made software. For each digitized image, additional software was used to reconstruct a smoothed outline and the midline of the fish. As described in greater detail in Jayne and Lauder (1995*a*), the midline was partitioned into lengths equaling the skull, individual vertebrae, the hypural bones and intervals one-fifth of the length of the caudal fin (Fig. 1). We obtained the anatomical dimensions necessary for partitioning the midline from X-ray photographs of each of the four fish used for statistical analysis (see Jayne and Lauder, 1995*a*).

Midline kinematic data were filtered with a low-pass (finite impulse response) filter with a cut-off frequency approximating 2–3 times the tail-beat frequency. From the reconstructed fish midlines, we determined the maximum amplitudes of the filtered values of lateral displacement (z_{max}) and the angle of lateral bending (β_{max}) between adjacent axial segments for seven longitudinal locations corresponding to the sites of the implanted electrodes as well as for reference points at the end of the vertebral column and near the trailing edge of the caudal fin (Fig. 1). Amplitudes of kinematic variables were measured as half of the difference between two successive maxima and minima during half of the tail-beat period; hence, during each cycle, values fluctuated between $\pm z_{max}$ and $\pm\beta_{max}$. For both z_{max} and β_{max} within each tail-beat cycle, lag times were calculated relative to the posterior end of the vertebral column and the other longitudinal locations, and these times were converted to units of phase (*z* phase, β phase) by dividing by the duration of the tail-beat cycle. For each longitudinal position, we also calculated the phase shift (*z*-β shift) between z_{max} and β_{max} such that negative values indicate that z_{max} preceded β_{max} (as described in Jayne and Lauder, 1995*a*).

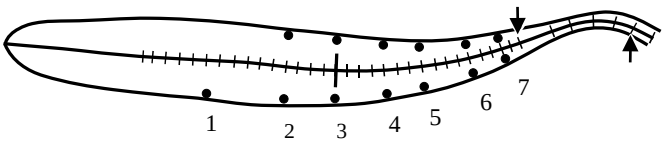

Fig. 1. Reconstructed outline and midline of *Micropterus salmoides* showing the longitudinal location of electrodes (dots; sites numbered). The left side of the fish is towards the bottom of the figure. The lines perpendicular to the midline indicate the longitudinal extent of the skull, individual vertebrae, hypurals and positions equaling one-fifth of the length of the caudal fin. The arrow pointing down indicates the joint between the hypurals and the most posterior vertebra. The arrow pointing up indicates the most posterior location (approximating maximum tail depth) used for kinematic analysis.

Electromyography

After anesthetizing the fish, we implanted a total of thirteen bipolar electrodes in superficial red muscle at the locations shown in Fig. 1 and Table 1. All thirteen channels were simultaneously used for recording during the experiments. Procedures for electrode construction and anesthesia are described in more detail in Jayne (1988) and Jayne and Lauder (1995*b*). We only analyzed results from electrodes that remained in position for the entire experimental period and after preservation. We used *post-mortem* dissections and X-ray photographs to confirm the exact location of each electrode relative to the axial skeleton.

Table 1. *Longitudinal locations of EMG electrodes for each of four individuals (1–4)*

	Fish 1		Fish 2		Fish 3		Fish 4		Mean	Joint	Mean
Site	L	R	L	R	L	R	L	R	joint	S.D.	length (*L*)
1			6		7		6		6.3	0.58	0.322
2	12	13	12	11	12	12	12	11	11.9	0.64	0.435
3	15	16	15	15	15	17	15	16	15.5	0.76	0.494
4	19	20	20	19	19	20	19	21	19.6	0.74	0.572
5	22	23	24	24	23	24	24	23	23.4	0.74	0.647
6	26	26	27	27	27	28	28	27	27.0	0.76	0.719
7	30	31	31	30	30	30	30	30	30.3	0.46	0.774
Tail											0.969

Locations are given in columns 2–9 as the numbers of the intervertebral joints (counting posteriorly from the skull) nearest the electrodes. L and R indicate left and right sides, respectively.
Mean joint values give the mean intervertebral joint electrode position for all four individuals and its standard deviation (joint S.D.).
Mean length indicates the longitudinal distance from each site to the snout expressed as a proportion of the total fish length (*L*).
The tail site was near the maximal span of the caudal fin (Fig. 1).

Electromyograms (EMGs) were amplified 20 000 times using Grass model P511 K preamplifiers using high- and low-bandpass filter settings of 100 Hz and 3 kHz, respectively, and a 60 Hz notch filter. The analog EMGs were recorded with a TEAC XR-5000 FM data recorder using a tape speed of 9.5 cm s^{-1}. A pulse generator provided coded output to both the NAC video system and the TEAC tape recorder, allowing synchronization of EMGs and video recordings. We converted the analog signal to a digital file using a sampling rate of 8 kHz (Jayne *et al.* 1990). We then filtered the digital EMGs using a finite impulse response filter that reduced the portion of the signal below 100 Hz to less than 10 % of its original amplitude.

To analyze the digitally filtered data, we used a custom-made computer program to determine the onset and offset times (to a resolution of ±1 ms) and the rectified integrated area of each EMG burst. Relative durations of EMG bursts were calculated by dividing the burst duration by the duration of the locomotor cycle, which was determined from lateral displacement data of the most posterior vertebra.

We used primarily four variables (see Table 2: on-β shift, off-β shift, on-*z* shift and off-*z* shift) to describe the timing of muscle activity relative to kinematic data. We subtracted the time of maximal convexity, β_{max} (towards the side of the fish containing the electrode) from the time of EMG onset, and the resulting difference was converted to a phase shift (on-β shift) by dividing by the cycle duration. In a similar fashion, we calculated the phase shift between EMG offset and the time at which a region was maximally concave towards the side of the electrode (off-β shift). Thus, values of zero for both on-β shift and off-β shift correspond to simple electrical activity during the shortening of contractile tissue. We also calculated the phase shift between the time of maximal lateral displacement (z_{max}) and EMG onset (on-*z* shift) and offset (off-*z* shift). For all lag time and phase shift variables, negative values indicate that the first event preceded the later event in the pair of events in a variable name. For example, a negative value of on-β shift indicates that EMG onset preceded the time of maximal lateral convexity.

Statistical analyses

We sought to obtain a complete set of results from seven longitudinal locations during each of five steady swimming speeds for all four individuals. However, because of the relatively small size of the superficial red muscle in *Micropterus salmoides* (Jayne and Lauder, 1995*b*; Johnson *et al.* 1994), we did not always obtain usable EMGs from every site shown in Fig. 1. Furthermore, a clear periodicity to the kinematic variables was not always evident since the amplitudes at site 1 (Fig. 1) at low speeds were occasionally near the limit of resolution of our movement data (approximately 0.25° of intervertebral flexion). Consequently, some descriptive statistics are included for site 1 when possible, but our primary statistical analysis (Table 2) was restricted to sites 2–7.

It is desirable to use statistical methods that account for individual variation, but for sites 2–7, we did not always have measurements for every individual at every speed. Thus, we analyzed our data with a two-way analysis of variance (ANOVA) with speed (five levels) and longitudinal location (six levels) as fixed and crossed factors. To minimize problems associated with pseudo-replication, we use only one mean value (N=3–4 tail beats) for each longitudinal location for each individual at each speed. If we obtained EMGs from both the left and right electrodes at a particular longitudinal location, we pooled left and right observations and used the resulting mean for our two-way ANOVAs. Because several ANOVAs were performed on the same series of results, a variety of methods should be considered for adjusting the criterion for deciding whether a test was statistically significant. We indicate where performing such a correction for multiple comparisons might alter the conclusions from our ANOVAs.

Table 2. *Summary of* F*-values from ANOVAs performed separately on each kinematic and EMG variable for sites 2–7*

Variable	Speed (4)	Site (5)	Speed × site (20)
Kinematic			
z_{max}	39.3 (<0.001)	121.7 (<0.001)	0.9 (0.61)
β_{max}	11.0 (<0.001)	117.6 (<0.001)	0.6 (0.90)
β phase	0.9 (0.40)	206.6 (<0.001)	0.6 (0.90)
z phase	1.3 (0.28)	729.3 (<0.001)	0.4 (0.99)
z-β shift	0.2 (0.92)	7.8 (<0.001)	2.5 (<0.001)
Electromyographic			
Duration (ms)	21.0 (<0.001)	5.1 (<0.001)	0.7 (0.80)
Duration (cycles)	0.6 (0.63)	17.5 (<0.001)	0.9 (0.63)
Intensity (%)	82.2 (<0.001)	1.9 (0.11)	0.4 (0.99)
EMG and kinematic			
On-β shift	4.6 (0.003)	5.4 (<0.001)	0.4 (0.99)
Off-β shift	3.1 (0.02)	26.5 (<0.001)	0.3 (0.99)
On-*z* shift	5.5 (0.001)	8.3 (<0.001)	0.6 (0.91)
Off-*z* shift	5.5 (0.001)	38.9 (<0.001)	0.8 (0.76)

P values are indicated parenthetically to the right of each value of *F*.

Degrees of freedom (d.f.) are to the right of each factor; error d.f. ranged from 68 to 90.

Results

Kinematics

General features of the kinematics of the *Micropterus salmoides* in this study conformed closely to those described previously for slightly larger individuals (Jayne and Lauder, 1995*a*). For the five standardized speeds, 0.7, 1.2, 1.6, 2.0 and 2.4 L s^{-1}, mean (N=4) values ± S.D. of the duration of the tail-beat cycle were 519±109, 394±59, 319±35, 278±34 and 247±46 ms, respectively. The corresponding tail-beat frequencies (f) ranged from 1.93 to 4.05 Hz and increased linearly with specific swimming speed (U), as described by the regression f=1.26U+1.05 (r^2=0.998, P<0.001).

Lateral displacement (z) and bending (β) (Fig. 2) were propagated posteriorly and varied with time in a sinusoidal fashion. For sites 2–7 (Fig. 1), which were used for the statistical analysis of EMGs, z_{max} and β_{max} increased significantly both with increased speed (most commonly from 0.7 to 1.6 $L\,s^{-1}$) and with increasingly posterior location (Table 2; Fig. 3A,B). As described previously (Jayne and Lauder, 1995*a*), z_{max} and β_{max} were not in phase, and the values of z-β shift changed significantly with site position (Table 2). When the phase of z_{max} and β_{max} for sites 2–7 was calculated relative to the end of the vertebral column, z phase and β phase were not significantly affected by speed (Table 2).

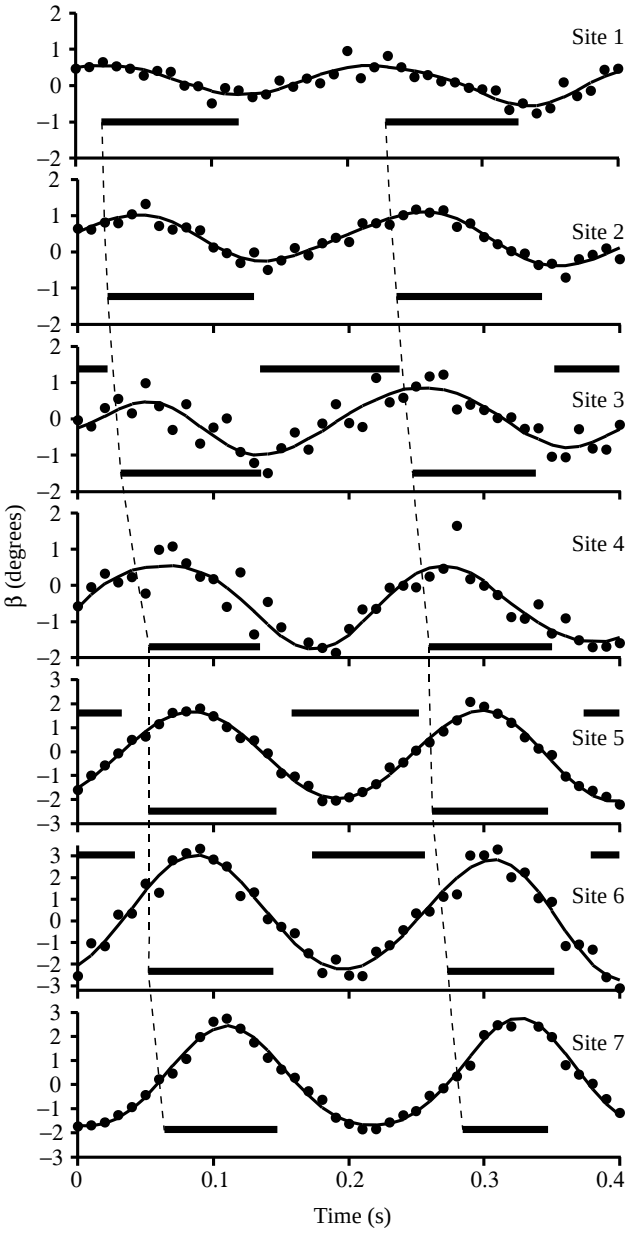

Fig. 2. Lateral vertebral flexion (β) and red muscle activity (horizontal black bars) *versus* time for a largemouth bass swimming at 2.4 $L\,s^{-1}$. The approximate longitudinal locations of the sites are as in Fig. 1. Lateral bending concave to the left and right are indicated by negative and positive values of β, respectively. The filled circles represent the unfiltered values of β, whereas the curves indicate values after low-pass filtering. The thick horizontal lines indicate red muscle activity with left- and right-side data shown below and above the plots of β, respectively. Data from the right-side electrodes at sites 2, 4 and 7 are not shown, since dissection revealed that these electrodes were not in the same body segment as those containing the left-side electrodes in this individual. The dashed lines connect the onset times of successive left-side EMGs. Note the progressive posterior increase in the phase shift of EMGs relative to lateral flexion.

Including kinematic data from the more extreme longitudinal locations of site 1 and the caudal fin (Fig. 1) in ANOVAs (results not shown in Table 2) of the kinematic phase and phase shift variables altered the conclusions regarding the significance of speed. For example, for values of z-β shift from site 1 through the caudal fin site, a two-way ANOVA revealed marginally significant effects of the speed (P=0.03) and of the speed×site (P=0.02) terms, whereas the effect of longitudinal position was highly significant (P<0.001), as had been the case for the results for sites 2–7 summarized in Table 2. When the phases of z_{max} and β_{max} were calculated relative to the caudal fin site rather than relative to the end of the vertebral column, the effect of longitudinal position was still highly significant (P<0.001) and the interaction terms were not significant; however, in this case, z phase (P=0.01) and β phase (P=0.002) decreased significantly with increased speed. Thus, analyses including site 1 and the caudal fin consistently showed more extensive effects of speed on kinematics than analyses confined to sites 2–7. However, because the primary goal of this study was to investigate congruent patterns of change in EMGs and kinematics with changing speed and longitudinal position, we concentrated the analysis on sites 2–7.

Electromyography

The fundamental pattern of red muscle activity consisted of posteriorly propagated EMGs that were unilateral and alternated between the left and right sides at a given longitudinal location (Fig. 4). The duration of EMGs (in ms) decreased significantly both with increased speed and with more posterior position within each swimming speed (Table 2). Relative EMG duration (in cycles) did not change significantly with swimming speed, but did decrease significantly with more posterior position (Table 2; Fig. 5). Using the relative EMG durations pooled for all available individuals (Fig. 5) at all five speeds, the mean values ± S.D. for sites 1–7 were 0.448±0.017, 0.451±0.016, 0.462±0.029, 0.432±0.010, 0.419±0.012, 0.403±0.022 and 0.335±0.043 cycles, respectively.

Noticeable variation did occur in the relative EMG durations among different tail beats within individual fish. For example, approximately 20 % of the observations for the relative EMG duration at sites 1–3 ranged from 0.5 to 0.53 cycles. An EMG duration exceeding 0.5 cycles implies some simultaneous activity of contralateral sites. However, when EMGs from a pair of contralateral electrodes were examined, there was never a consistent pattern of bilateral activity. In contrast to the more

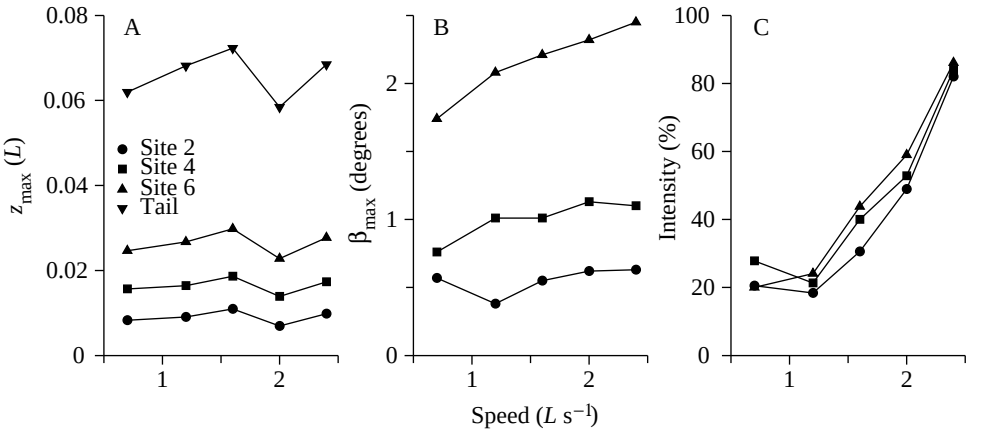

Fig. 3. Mean values of maximal lateral displacement z_{max} (A), maximal lateral vertebral flexion β_{max} (B) and the intensity of red muscle EMG activity (C) *versus* swimming speed. Note that, within a single cycle, amplitudes of kinematic variables fluctuate between $\pm z_{max}$ and $\pm \beta_{max}$. EMG intensity is shown relative to the greatest value observed for a single EMG burst for swimming speeds ranging from 0.7 to 2.4 $L\,s^{-1}$. Values for sites 2, 4 and 6 are cell means from ANOVAs (Table 2) performed on the means from each of four individuals.

anterior sites, relative EMG durations at sites 4–7 never exceeded half a cycle. Furthermore, for the most posterior position (site 7), all values of relative duration (with the exception of one) were less than 0.39 cycles.

The relative intensity of red muscle activity increased significantly with increased swimming speed, and the pattern of change in relative intensity with speed was similar for all longitudinal positions (Table 2; Fig. 4). EMG intensity increased by approximately fourfold between swimming speeds of 0.7 and 2.4 $L\,s^{-1}$ (Fig. 3C), whereas the amplitudes

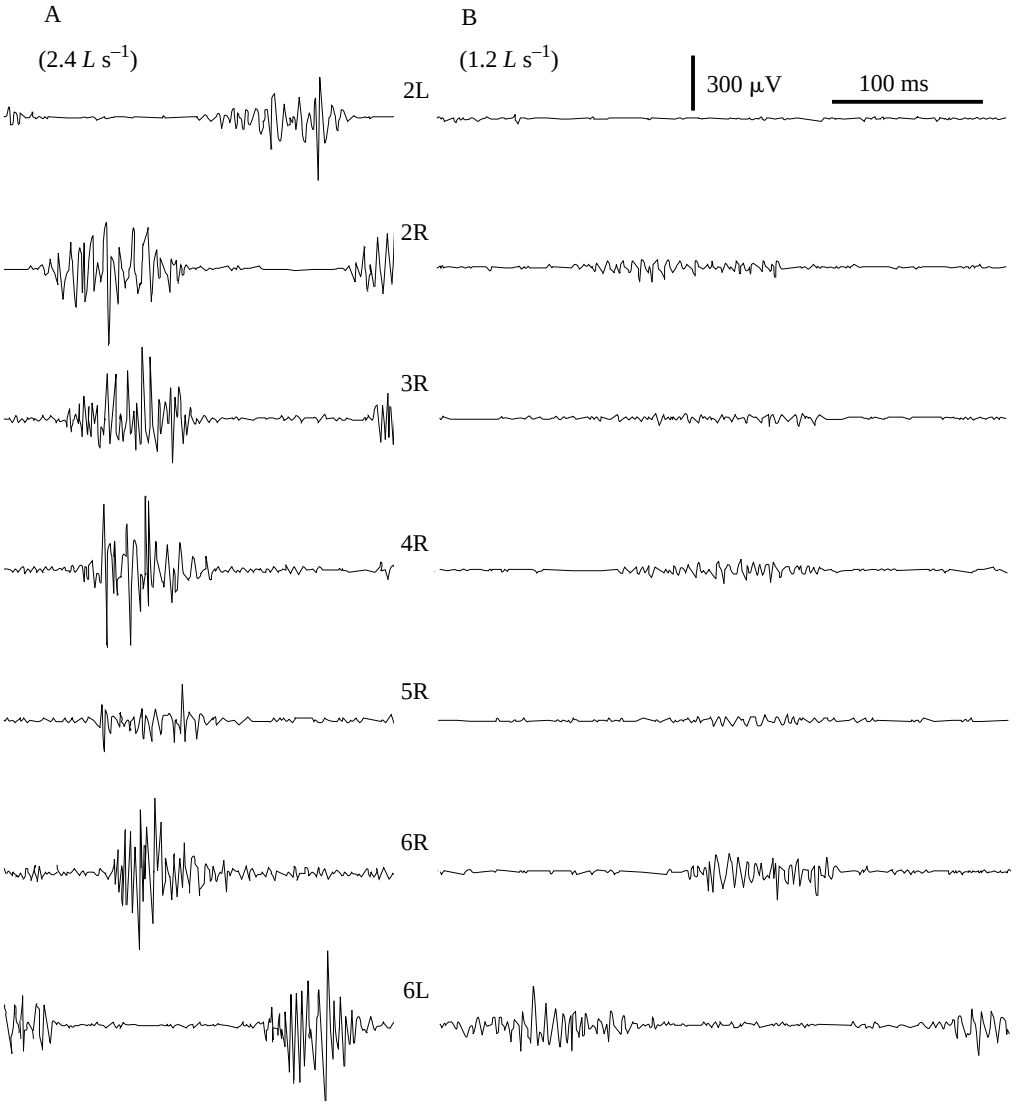

Fig. 4. EMGs from the superficial red muscle of a single *Micropterus salmoides* swimming at speeds of 2.4 (A) and 1.2 $L\,s^{-1}$ (B). The time and voltage scales are identical for all channels. For each channel, numbers indicate the longitudinal location of the recording site, with 1 being most anterior (Fig. 1), and R and L indicate right and left sides, respectively.

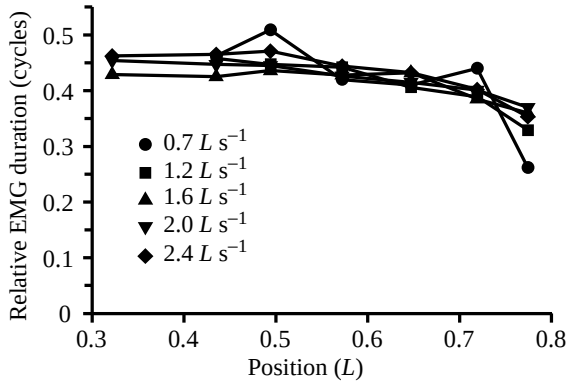

Fig. 5. Mean values of the relative duration of red muscle EMGs. Position indicates the proportion of total length (L) of a site posterior to the snout of the fish. Values are based on observations from a maximum of four individuals. Note that the values for the most anterior site (site 1, 0.322L) were not included in the ANOVAs, which are summarized in Table 2, as accurately measurable activity was not consistently found at anterior sites during slow-speed swimming (e.g. Fig. 4B: site 2L). Relative EMG duration at sites 2–7 showed a significant decrease posteriorly but was unaffected by swimming speed.

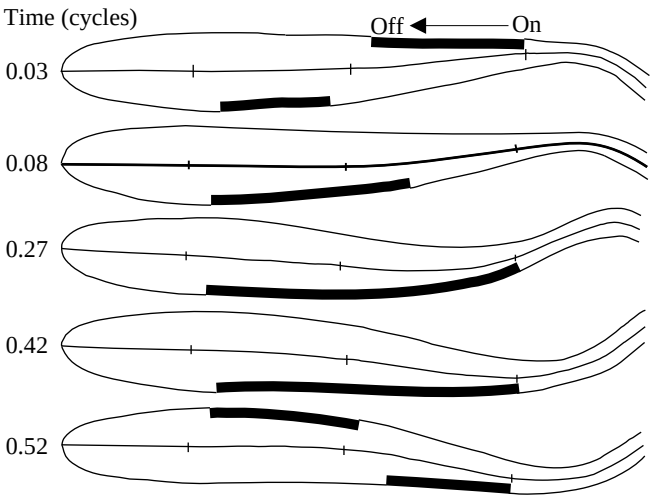

Fig. 6. Summary of red axial muscle activity of *Micropterus salmoides* based on direct observation from 13 recording sites (Fig. 1) in one individual swimming at $2.4\,L\,s^{-1}$ and with a cycle duration of 303 ms. Outlines of the fish were taken directly from digitized video images. The three reference marks on the midline of the fish indicate the posterior border of the skull, the joint between the trunk and the caudal vertebrae, and the most posterior intervertebral joint. The thick lines along the sides of the fish indicate muscle activity. Note that, because muscle activity is propagated posteriorly, the posterior end of the thick line indicates the onset of muscle activity and the anterior end indicates activity immediately prior to offset.

of kinematic variables only increased by as much as 50 % over the same speed range (Fig. 3A,B). EMG intensity also did not appear to be asymptotically approaching a maximum near $2.4\,L\,s^{-1}$ (Fig. 3C). In contrast, the most conspicuous increase in z_{max} occurred between 0.7 and $1.6\,L\,s^{-1}$ (Fig. 3A), and for β_{max}, most longitudinal positions also showed reduced rates of increase between 2 and $2.4\,L\,s^{-1}$ (Fig. 3B).

Despite the fact that muscle activity propagated posteriorly, there were usually periods when the entire longitudinal extent of the red muscle on one side of the fish was simultaneously active (Fig. 6). The longitudinal extent of muscle activity can also be seen in Fig. 7 by observing the number of longitudinal positions for which EMGs (the horizontal bars) intersect a line (representing an instant in time) that is perpendicular to the x-axis. Using the mean values for experimentally observed muscle activity (Fig. 7C–E), the durations of simultaneous ipsilateral activity of sites 1–7 for speeds from 1.6 to $2.4\,L\,s^{-1}$ were 20 ms (0.062 cycles), 50 ms (0.179 cycles) and 46 ms (0.247 cycles), respectively. The timing of muscle activity at site 1 could not be determined with confidence for 0.7 and $1.2\,L\,s^{-1}$ (Fig. 7A,B). Using data from site 2, extrapolated to obtain estimated values for site 1 at the two slowest swimming speeds (Fig. 7A,B), the durations of simultaneous ipsilateral activity for 0.7 and $1.2\,L\,s^{-1}$ were 0 and 22 ms (0.055 cycles), respectively. Thus, the proportion of the locomotor cycle with simultaneous ipsilateral muscle activity tended to increase from site 1 to site 7 with increased swimming speed. Simultaneous activity from sites 1–7 on one side of the fish generally began close to the time when the trailing edge of the tail was maximally displaced to the contralateral side (see Fig. 6 at 0.27 cycles) and ended near or before the time when the tail was crossing the axis of forward progression.

The timing of muscle activity relative to kinematics is complicated by the fact that all phase-shift variables relating muscle activity to kinematics varied significantly with both speed and longitudinal position (Table 2: on-β shift, off-β shift, on-z shift and off-z shift). The time difference between EMGs and kinematic events generally showed a progressive posterior increase within each of the swimming speeds (Fig. 8).

If the timing of EMGs corresponded exactly to shortening of contractile tissue (as predicted from lateral bending), then both on-β shift and off-β shift would equal zero. As shown in Fig. 8A,B, anterior EMG onset was nearly synchronous with the time when a region was maximally convex towards the side with the recording electrode (on-β shift=0). Mean values of on-β shift were as large as -0.170 cycles for the most posterior sites at the fastest swimming speed (Fig. 8A), and faster swimming speeds generally had greater on-β shift values. If EMG duration were constant among different longitudinal locations, then one would expect that longitudinal variation in off-β shift would resemble that of on-β shift. However, the longitudinal variation in EMG duration is such that it exaggerates the progressive posterior increase in amplitudes of off-β shift compared with on-β shift. For example, at site 7, mean values of on-β shift ranged from -0.065 to -0.170 cycles, whereas off-β shift ranged from -0.239 to -0.317 cycles.

The phase-shift variables do not indicate whether there is a constant time lag between muscle activity and kinematic events

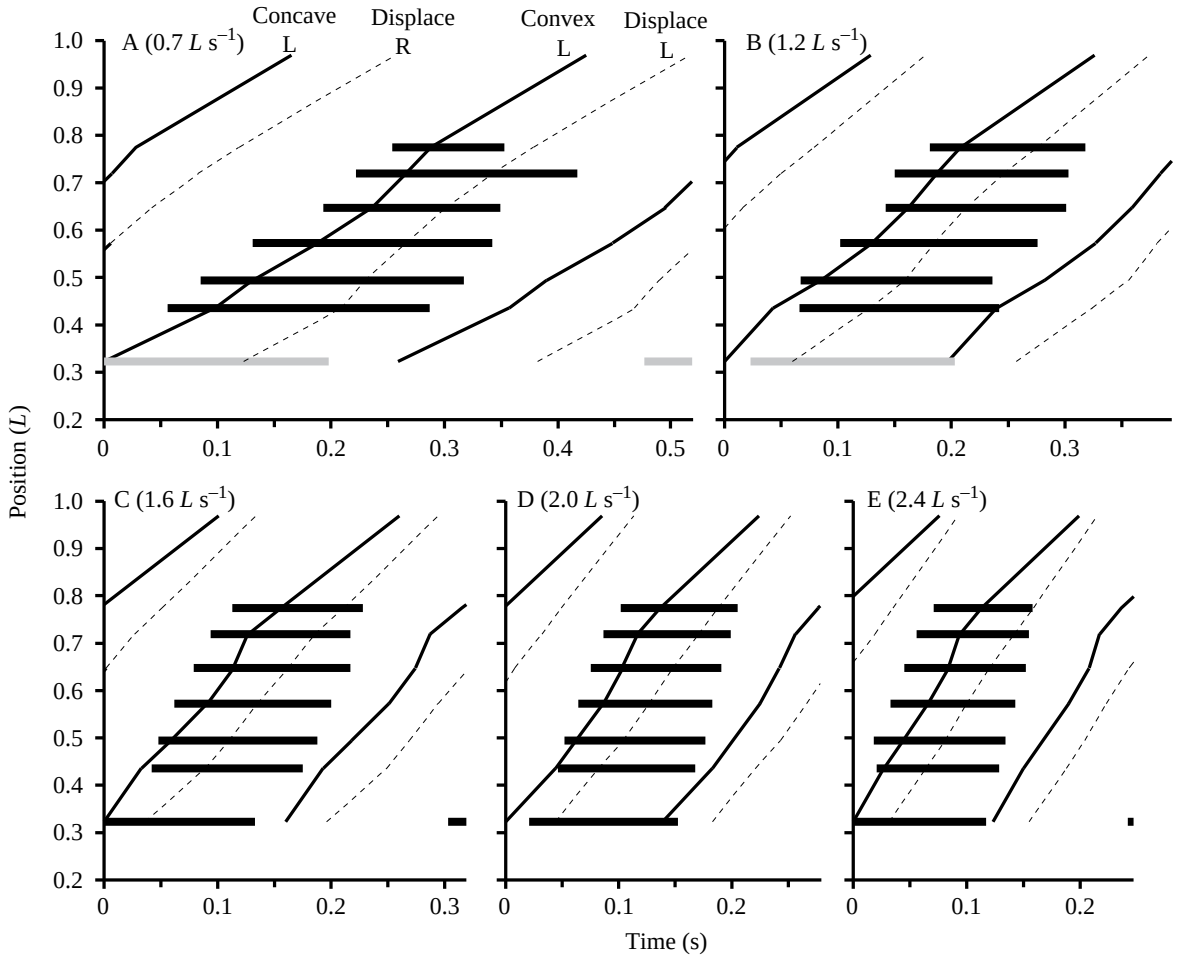

Fig. 7. Mean values for the timing of EMGs and kinematic events for relative swimming speeds of 0.7 (A), 1.2 (B), 1.6 (C), 2.0 (D) and 2.4L s^{-1} (E). A time interval equal to one cycle is shown for each panel and zero equals the time at which the most anterior electrode location (site 1, Fig. 1) is bent maximally convex to the left. The ordinate of each plot indicates longitudinal position as the distance from the snout to sites along the midline in units of total length of the fish. The thick horizontal bars indicate left-side muscle activity and are for sites 1–7 from the bottom to the top of the figure. The stippled horizontal bars are used for the timing of the site 1 EMG where this was estimated from the mean values of relative duration and on-β shift obtained for site 2 at the same swimming speed. The solid oblique lines indicate the time of maximal lateral flexion and the dashed oblique lines indicate maximal lateral displacement to the left (L) and right (R). Note that all figures are shown with the *x*- and *y*-axes to the same scale. Hence, a greater slope indicates a faster speed of posterior propagation of events along the longitudinal locations. In A and B, some of the irregularities in the pattern of muscle activity (e.g. long EMG duration at 0.7L) are the result of mean values that were calculated from fewer than four individuals.

because the cycle duration changes with swimming speed. Consequently, we also analyzed the lags (in ms) between EMGs and lateral bending and displacement. Two-way ANOVAs (not shown in Table 2) demonstrated that all four EMG–kinematic lag variables (on-β lag, off-β lag, on-*z* lag and off-*z* lag) had highly significant differences attributable to both swimming speed and longitudinal position, with a pattern of variation grossly similar to that observed for the phase-shift variables (compare Fig. 8A,B with Fig. 8C,D).

As shown in Fig. 8C, mean values of on-β lag ranged from −57 ms to 25 ms, and roughly 90 % of the values for sites 4–7 (0.572–0.774L) ranged from −45 ms to −25 ms. Values of off-β lag ranged from −156 ms to 8 ms, and approximately 90 % of the values for sites 4–7 were less than −50 ms (Fig. 8D). Interestingly, the greatest disparity of EMG phase relative to β occurred for the fastest speed (Fig. 8A,B), whereas the greatest lag times between EMGs and bending generally occurred for the slowest swimming speed (Fig. 8C,D). The phase shifts and time lags between EMGs and lateral displacement showed overall patterns of change associated with swimming speed and longitudinal position similar to those for the timing of EMGs relative to lateral bending (Fig. 7).

Longitudinal propagation of kinematics and EMGs

We were not always able to record EMGs simultaneously from adjacent ipsilateral sites, but we commonly did obtain EMGs from most of the longitudinal positions as a result of having electrodes in both the left and right sides. Thus, to allow pooling of EMG results from the left and the right sides, we added values of on-β shift to those of β phase to obtain the

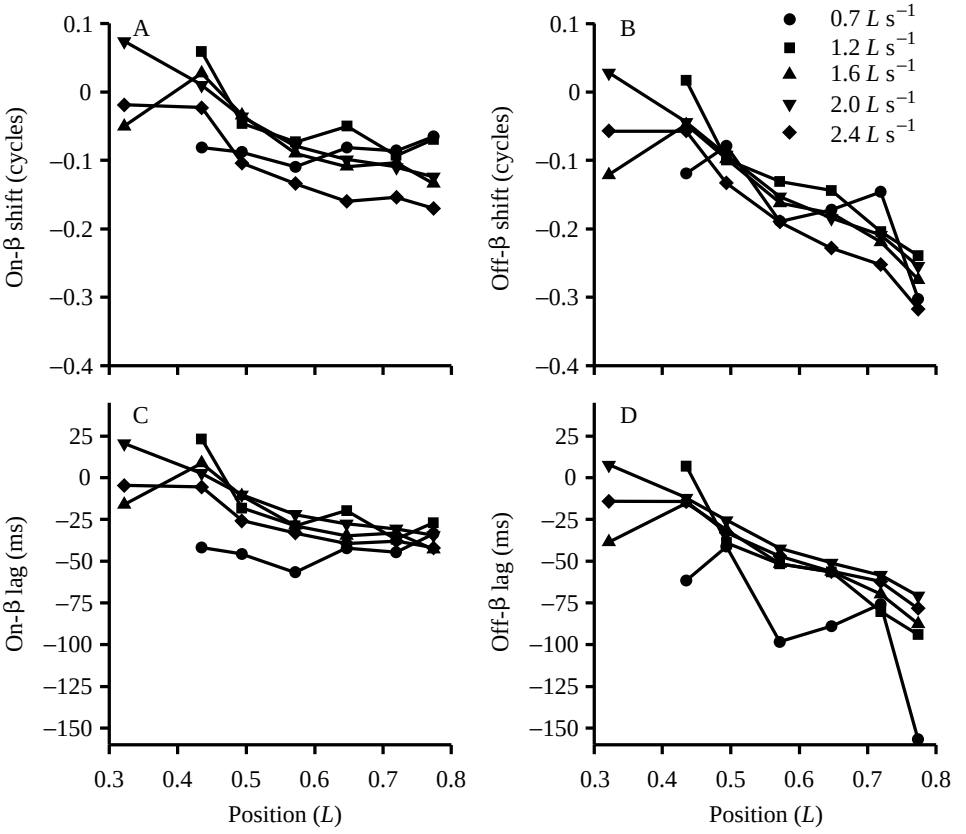

Fig. 8. Mean timing of EMG onset and offset relative to lateral vertebral bending (β). All values are based on observations from a maximum of four individuals. The timing of EMG onset is relative to the time at which the region of the electrode is maximally convex towards the side of the recording site, whereas offset times are relative to the time of maximal concavity. Phase shifts (in cycles) between EMGs and lateral flexion are shown in A and B, whereas C and D show lag times (in ms). Note that data shown above for the most anterior position (site 1, 0.322*L*) were not included in the ANOVAs summarized in Table 2.

phase of EMG onset, and then, for each successive pair of adjacent longitudinal locations, we obtained the phase difference and divided it by the number of intervening body segments (calculated separately for each individual fish). The resulting intersegmental phase lags (in cycles per body segment) provide a useful indication of the time course of events, and the inverse indicates a standardized rate of propagation (also referred to as EMG wavelength) in terms of numbers of body segments per cycle. Similar calculations were performed for EMG offsets. Calculations of intersegmental phase lags for kinematic variables were simpler (used left-side data only) since there were no missing values.

Neither the intersegmental phase lags (IPL) for lateral displacement (z) nor those for lateral bending (β) changed significantly with swimming speed (Table 3). z IPL did have highly significant variation among longitudinal locations (Table 3), with the smallest values consistently occurring at intermediate longitudinal locations (Fig. 9A). The mean z IPL for all data pooled for sites 2–6 was 0.0195 cycles segment^{-1}. Mean values (pooled across all speeds) of z IPL for sites 1–2 and for sites 6–7 were 0.0289 and 0.0257 cycles segment^{-1}, respectively. Values of β IPL had marginally significant variation with longitudinal position (Table 3) which was no longer significant if a Bonferroni correction was made for multiple comparisons (P=0.003). Values of β IPL generally decreased posteriorly (Fig. 9B). Using pooled values from all swimming speeds, mean values of β IPL from sites 2–3 and sites 5–6 were 0.0255 and 0.0135 cycles segment^{-1}, respectively.

The intersegmental phase lags of EMG onset and offset showed no highly significant (Table 3) or consistent pattern (Fig. 9C,D) of variation with either longitudinal position or swimming speed. Using data pooled for all swimming speeds from sites 2–7 (Fig. 9, N=25), mean ± S.E.M.values of IPL for EMG onset and offset were 0.0182±0.0020 and 0.0102±0.0018 cycles segment^{-1}, respectively. Despite the rather high variability in the estimates of IPL for EMGs (Fig. 9C,D), onset IPL was significantly greater than offset IPL (paired t-test, t=4.18, d.f.=24, P<0.001). Hence, as indicated by the inverse

Table 3. *Summary of* F*-values from ANOVAs performed on intersegmental phase lags (IPL) for sites 2–7*

IPL variable	Speed (4)	Site (4)	Speed × site (16)
β	0.70 (0.592)	3.58 (0.010)	0.62 (0.859)
z	0.33 (0.858)	7.44 (<0.001)	0.46 (0.956)
EMG onset	2.31 (0.070)	2.32 (0.069)	8.85 (0.631)
EMG offset	1.53 (0.026)	2.36 (0.065)	1.18 (0.318)

P values are indicated parenthetically to the right of each value of F.

Degrees of freedom (d.f.) are shown to the right of each factor, and error d.f. ranged from 52 to 70.

Cell means are shown in Fig. 9.

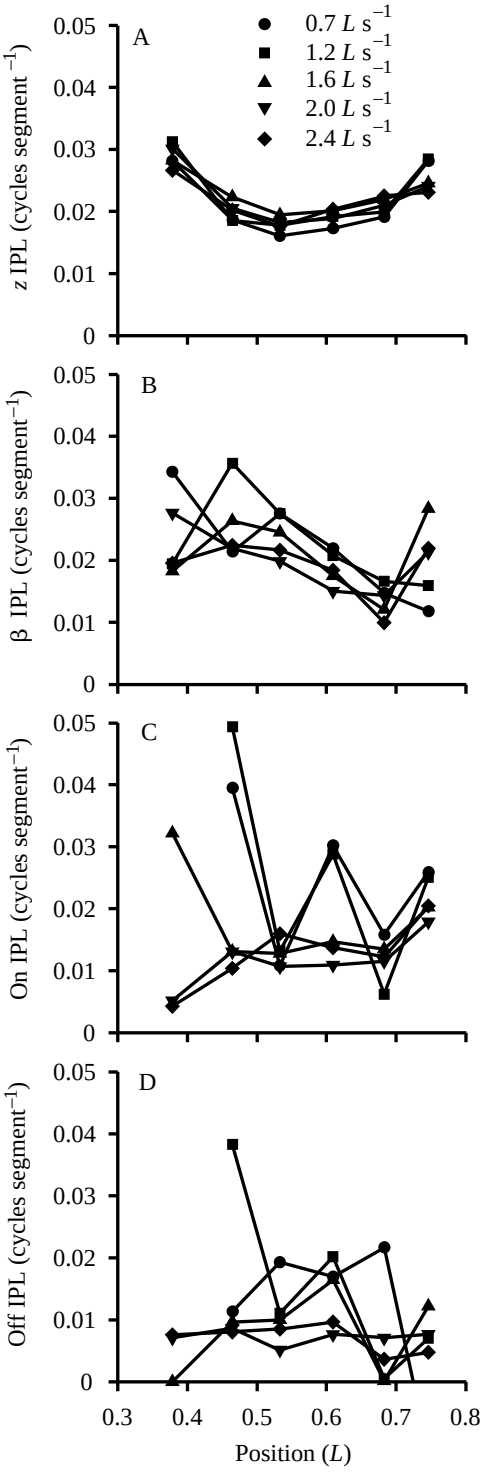

Fig. 9. Mean values of intersegmental phase lags (IPL) for lateral displacement (A), lateral bending (B), EMG onset (C) and EMG offset (D). Position indicates the mean longitudinal distance from the snout using the two values from the pair of sites for which phase differences were calculated and divided by the number of intervening body segments. See Table 3 for results of ANOVAs and note that the most anterior location (site 1, 0.322*L*) was not included in the ANOVAs. All axes in all panels are to the same scale. Note that one value (−0.01) is not shown for the most posterior location at the slowest speed in D.

of the mean values of IPL, EMG offsets propagated posteriorly faster than EMG onsets (98 *versus* 55 segments per cycle).

Similar paired comparisons can be made between values of IPL for EMGs and kinematic events. For the two slowest swimming speeds, smaller sample sizes of EMG intersegmental phase lags contributed to a large among-site variance, which obscured most trends for paired comparisons between EMG and kinematic intersegmental phase lags (Fig. 9). However, when comparisons were restricted to the more precise data from the three fastest speeds, some interesting differences in IPL became apparent. For example, for the three fastest swimming speeds, the values of IPL for β (Fig. 9B) were significantly larger than those for EMG onset (Fig. 9B *versus* Fig. 9C, paired *t*-test, t=4.62, d.f.=14, P<0.001). Thus, EMG onset propagated faster than lateral bending at homologous longitudinal locations. For this comparison, the disparity in values of IPL was greatest anteriorly and diminished posteriorly until, near site 6, the values of IPL were nearly identical. Similarly, for the three fastest speeds, the values of IPL for EMG offset (Fig. 9D) were smaller than those of β (Fig. 9B) and the difference between these two quantities increased anteriorly along the fish.

Discussion

Currently, only limited comparative data are available for the intersegmental phase lags of EMGs during the undulatory swimming of vertebrates. For a combination of intact and fictive preparations of anguilliform swimmers, EMG intersegmental phase lags generally approximate 0.01 cycles segment^{-1} and appear to be unaffected by either longitudinal position or cycle duration (Grillner and Kashin, 1976; Wallén and Williams, 1984). For fictive preparations of dogfish (Grillner, 1974, calculated from his Fig. 5A) and goldfish (Fetcho and Svoboda, 1993), EMG intersegmental phase lags approximated 0.004 and 0.021 cycles segment^{-1}, respectively, and these values and did not vary with frequency of EMGs. Consequently, our study of *Micropterus salmoides* and all other studies of fish swimming currently support the generalization that EMG intersegmental phase lags are independent of swimming speed.

For the swimming of intact trout, Williams *et al.* (1989) found that the rate of EMG propagation depended on longitudinal position, with anterior locations having faster speeds of propagation; however, the propagation speeds of lateral bending appeared to be constant along the entire length of the fish. Williams *et al.* (1989) expressed rates of propagation in the trout in terms of percentage length rather than body segments; therefore, direct comparisons of intersegmental phase lags are not possible for the trout and *Micropterus salmoides*. Data from studies of trout and carp (Williams *et al.* 1989; van Leeuwen *et al.* 1990) suggest that the propagation of EMG offset is faster than that of EMG onset in both taxa (Fig. 10). Hence, bass, trout and carp, which are all subcarangiform swimmers, appear to have different propagation speeds of EMG onset and offset, whereas available

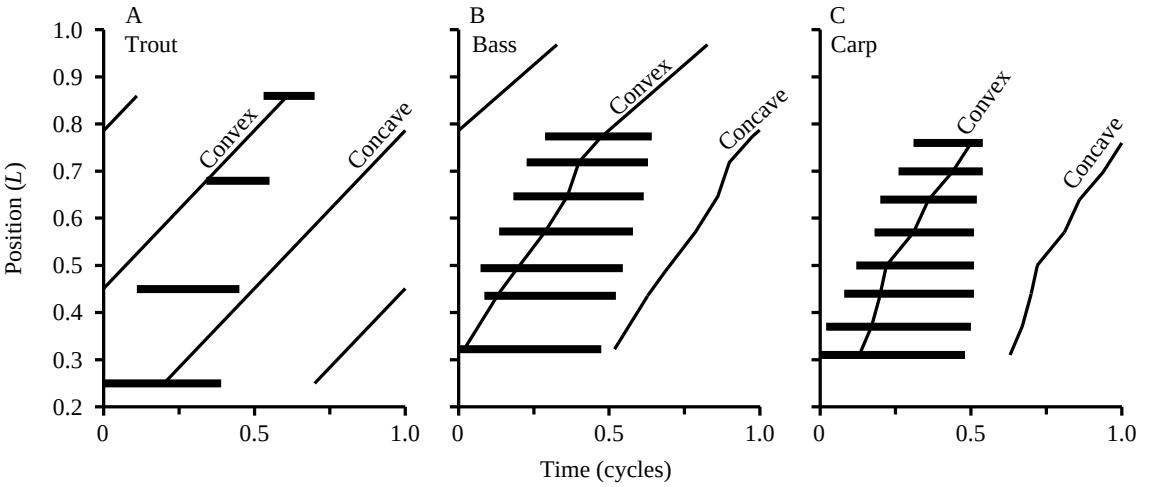

Fig. 10. Comparative summary of bending and red muscle activity for steady swimming of fishes. (A) Trout data were modified from Williams *et al.* (1989, Fig. 1) for a fish with L=28 cm and a swimming speed of $0.64\,L\,s^{-1}$. (B) Mean values for largemouth bass swimming at $2.4\,L\,s^{-1}$. (C) Carp data were modified from van Leeuwen *et al.* (1990, Fig. 4) for a fish with L=17.9 cm and a swimming speed of $1.73\,L\,s^{-1}$. The thick horizontal bars indicate the timing of red axial muscle activity for different longitudinal locations within each fish. All figures have been standardized so that time 0 equals the onset of muscle activity at the most anterior recording site. Lateral flexion is indicated relative to the side of the fish from which muscle activity was observed. Thus, muscle activity between the times of maximal convexity and maximal concavity corresponds to electrical activity during the shortening of the contractile tissue.

data for diverse anguilliform swimmers appear to indicate that EMG onsets and offsets propagate with the same speed (Grillner and Kashin, 1976; Williams *et al.* 1989; Jayne, 1988).

We designed our experiments specifically to detect effects of speed and longitudinal location on the relationship of EMGs to movement. Consequently, we found effects of speed on certain variables which have previously been found to be constant with speed in addition to finding effects of speed on other variables which have not been previously quantified. For example, for the steady swimming of trout, Williams *et al.* (1989) found that speed did not affect the timing of EMGs relative to lateral bending, although this relationship did vary longitudinally. In contrast, for *Micropterus salmoides*, the timing of EMGs relative to lateral bending varied significantly both with speed and with longitudinal location (Table 2), regardless of whether values were expressed as lag times or as phase shifts (Fig. 8). In the caudal regions of *Micropterus salmoides*, values of on-β shift (Fig. 8A) changed by as much as 0.105 cycles between 0.7 and $2.4\,L\,s^{-1}$, while values of on-β lag were generally between −30 and −40 ms (Fig. 8C). Values of off-β shift changed with speed similarly to those of on-β shift. At a given longitudinal location, values of off-β lag were larger than those of on-β lag, and most off-β lags ranged from −50 to −100 ms.

For *Micropterus salmoides*, Johnson *et al.* (1994) found that the times to peak tension and half-relaxation for isometric twitch were 43 and 67 ms, respectively, for *in vitro* samples of red muscle removed near sites 6–7 (Fig. 1) and tested at 20 °C. Interestingly, the disparity between the times of EMG onset and the time of maximal convexity was nearly always less than the time to peak tension for the superficial red muscle. For other species of fish that swim using the subcarangiform mode, considerable longitudinal variation may occur for the time course of force development and relaxation. For superficial red muscle of the scup, Rome *et al.* (1993) found that the relaxation time could increase nearly twofold posteriorly. From the available data on the fast axial musculature of fish, it appears that the times of both force development and relaxation tend to increase posteriorly, but the magnitude of longitudinal changes in relaxation times generally exceeds that of the times required to develop tension (Wardle, 1985; Davies and Johnston, 1993; Altringham *et al.* 1993). Because these previously described patterns of longitudinal variation in contractile properties are remarkably congruent with the longitudinal patterns of variation which we found for values of on-β lag and off-β lag (Fig. 8C,D), it is tempting to conclude that the timing differences between force and lateral bending are minimal compared with differences in the timing of electrical activity and lateral bending. This suggestion may be further supported by observations of positive *in vitro* work loops for the superficial red muscle of *Micropterus salmoides* using strains and stimulation phases representative for a very posterior location (site 6–7) during steady swimming (Johnson *et al.* 1994). Because not all species of fish appear to show longitudinal variation in contractile properties, and both strain and stimulus have complex effects on force development and relaxation (Johnston *et al.* 1993), further experiments clarifying the extent of longitudinal variation in the contractile properties of *Micropterus salmoides* muscle would be very desirable.

The strain of the superficial red muscle of *Micropterus salmoides* can be estimated by converting values of β_{max} to a percentage length change, as described previously by Jayne and Lauder (1995*a*). Values of β_{max} in the present study were statistically indistinguishable (two-tailed paired t-test, t=0.72, d.f.=15, P=0.48) from those published previously for

Table 4. *Mean values of maximal lateral bending and associated estimates of strain for the superficial red muscle of* Micropterus salmoides

Site	Variable	Speed ($L\,s^{-1}$) 0.7	1.2	1.6	2.0	2.4
1	β_{max} (degrees)	0.66 (0.38)	0.55 (0.37)	0.68 (0.17)	0.63 (0.12)	0.57 (0.31)
	Strain (±%)	2.7	2.3	2.8	2.6	2.3
2	β_{max} (degrees)	0.57 (0.24)	0.38 (0.20)	0.55 (0.16)	0.62 (0.07)	0.63 (0.18)
	Strain (±%)	2.8	1.9	2.7	3.1	3.1
3	β_{max} (degrees)	0.52 (0.13)	0.65 (0.16)	0.75 (0.14)	0.85 (0.04)	0.88 (0.15)
	Strain (±%)	2.4	3.0	3.5	3.9	4.1
4	β_{max} (degrees)	0.76 (0.36)	1.01 (0.22)	1.01 (0.14)	1.13 (0.19)	1.1 (0.07)
	Strain (±%)	3.0	4.0	4.0	4.4	4.3
5	β_{max} (degrees)	1.17 (0.60)	1.39 (0.28)	1.58 (0.12)	1.81 (0.30)	1.68 (0.21)
	Strain (±%)	4.1	4.9	5.5	6.4	5.9
6	β_{max} (degrees)	1.74 (0.50)	2.08 (0.30)	2.21 (0.24)	2.32 (0.23)	2.45 (0.16)
	Strain (±%)	4.8	5.8	6.2	6.4	6.8
7	β_{max} (degrees)	1.53 (0.46)	1.85 (0.42)	2.03 (0.40)	2.21 (0.27)	2.09 (0.23)
	Strain (±%)	3.4	4.2	4.6	5.0	4.7

All means are based on N=4 individuals.
Site indicates longitudinal position as illustrated in Fig. 1.
Values are means (S.D.).
Strain was calculated by converting values of β_{max} to percentage length changes as described by Jayne and Lauder (1995*a*).

Micropterus salmoides swimming steadily unencumbered by electrodes (present study Table 4 using sites 2, 3, 4 and 6 *versus* Jayne and Lauder, 1995*a*, Table 4). Consequently, our methodology for obtaining EMGs appeared to have few obvious effects on the swimming behavior of *Micropterus salmoides* over the observed range of swimming speeds. As shown in Table 4, estimated strains of the superficial red muscle were between ±1.9 % and ±6.8 % depending on the exact longitudinal location and swimming speed. Besides agreeing well with our previous observations for *Micropterus salmoides* (1.7–6.6 %; Jayne and Lauder, 1994*a*), these estimates of superficial red muscle strain are very similar to values presently available for the steady swimming of a variety of other fish species (van Leeuwen *et al.* 1990; Rome and Swank, 1992; Rome *et al.* 1993).

Fairly detailed comparisons are now possible for the timing of red muscle activity and lateral bending for *Micropterus salmoides*, the trout (Williams *et al.* 1989) and the carp *Cyprinus carpio* (van Leeuwen *et al.* 1990), and this information is summarized in Fig. 10, which shows EMGs and kinematic data plotted on a time scale standardized to equal the duration of a single cycle. The largemouth bass appears to be more similar to the carp for two main reasons. First, in both bass and carp, EMG onsets occur before the time of maximal convexity, whereas in the anterior region of the trout the EMGs lag behind this kinematic event. Second, in both bass and carp, there is a noticeable portion of the locomotor cycle for which all of the red muscle was simultaneously activated on one side of the fish, whereas the greatest longitudinal extent of simultaneous ipsilateral muscle activity in the trout is always less than its body length. As discussed earlier, decreased swimming speed may decrease the longitudinal extent of muscle activity in *Micropterus salmoides*, and data shown in Fig. 10 are for a trout swimming more slowly than the bass. However, Williams *et al.* (1989) reported that this pattern of muscle activation was also characteristic of faster swimming speeds. In the light of the substantial effects of speed on EMGs and their relationships to kinematics in *Micropterus salmoides*, future comparisons will best be accomplished using standardized swimming speeds for different fish taxa.

Similar numbers of vertebrae are found in both bass (30–32) and carp (35–36), whereas trout (60–66) have nearly twice as many (Scott and Crossman, 1973). Consequently, similar numbers of vertebrae may be a key factor contributing to the similar muscular control of swimming movements in bass and carp. Bass, carp and trout may all be considered subcarangiform swimmers, and the overall shape of moderately sized individuals from all three species resembles the generalized fusiform condition (Webb, 1994). Because high numbers of vertebrae are often correlated with elongate shape, these two factors are often confounding when attempting to interpret the diversity of fish swimming modes and their underlying muscular basis. In the light of these encouraging results comparing bass with carp and trout, interpreting the diversity of morphology and swimming modes in fishes should be facilitated by additional studies that attempt to isolate the effects of additional morphological traits (such as variation in body depth) when numbers of vertebrae are similar

(e.g. by comparing *Micropterus salmoides* and *Lepomis macrochirus* motor and kinematic patterns).

We are grateful to J. Seigel and the Section of Fishes at the Los Angeles County Museum for the X-ray photographs of specimens. H. Nguyen, J. Davis, A. Lozada and B. Malas laboriously digitized the video images. Support was provided by NSF grants BNS 8919497 to B.C.J. and G.V.L., and NSF BSR 9007994 to G.V.L. The high-speed video system was obtained under NSF BBS 8820664.

References

ALTRINGHAM, J. D. AND JOHNSTON, I. A. (1990). Scaling effects on muscle function: power output of isolated fish muscle fibres performing oscillatory work. *J. exp. Biol.* **151**, 453–467.

ALTRINGHAM, J. D., WARDLE, C. S. AND SMITH, C. I. (1993). Myotomal muscle function at different locations in the body of a swimming fish. *J. exp. Biol.* **182**, 191–206.

BLIGHT, A. R. (1977). The muscular control of vertebrate swimming movements. *Biol. Rev.* **52**, 181–218.

BONE, Q. (1966). On the function of the two types of myotomal muscle fibre in elasmobranch fish. *J. mar. biol. Ass. UK* **46**, 321–349.

BONE, Q., KICENIUK, J. AND JONES, D. R. (1978). On the role of the different fibre types in fish myotomes at intermediate swimming speeds. *Fishery Bull. Fish. Wildl. Serv. U.S.* **76**, 691–699.

DAVIES, M. AND JOHNSTON, I. A. (1993). Muscle fibres in rostral and caudal myotomes of the Atlantic cod have different contractile properties. *J. Physiol., Lond.* **459**, 8P.

FETCHO, J. R. AND SVOBODA, K. R. (1993). Fictive swimming elicited by electrical stimulation of the midbrain in goldfish. *J. Neurophysiol.* **70**, 764–780.

GRILLNER, S. (1974). On the generation of locomotion in the spinal dogfish. *Expl Brain Res.* **20**, 459–470.

GRILLNER, S. AND KASHIN, S. (1976). On the generation and performance of swimming in fish. In *Neural Control of Locomotion* (ed. R. M. Herman, S. Grillner, P. S. G. Stein and D. G. Stuart), pp. 181–201. New York: Plenum Press.

HUDSON, R. C. L. (1973). On the function of the white muscles in teleosts at intermediate swimming speeds. *J. exp. Biol.* **58**, 509–522.

JAYNE, B. C. (1988). Muscular mechanisms of snake locomotion: an electromyographic study of lateral undulation of the Florida banded water snake (*Nerodia fasciata*) and the yellow rat snake (*Elaphe obsoleta*). *J. Morph.* **197**, 159–181.

JAYNE, B. C. AND LAUDER, G. V. (1993). Red and white muscle activity and kinematics of the escape response of the bluegill sunfish during swimming. *J. comp. Physiol.* A **173**, 495–508.

JAYNE, B. C. AND LAUDER, G. V. (1994*a*). How fish use slow and fast muscle fibers: implications for models of vertebrate muscle recruitment. *J. comp. Physiol.* A **175**, 123–131.

JAYNE, B. C. AND LAUDER, G. V. (1994*b*). Comparative morphology of the myomeres and axial skeleton in four genera of centrarchid fishes. *J. Morph.* **220**, 185–205.

JAYNE, B. C. AND LAUDER, G. V. (1995*a*). Speed effects on midline kinematics during steady undulatory swimming of largemouth bass, *Micropterus salmoides*. *J. exp. Biol.* **198**, 585–602.

JAYNE, B. C. AND LAUDER, G. V. (1995*b*). Are muscle fibers within fish myotomes activated synchronously? Patterns of recruitment within deep myomeric musculature during swimming in largemouth bass. *J. exp. Biol.* **198**, 805–815.

JAYNE, B. C., LAUDER, G. V., REILLY, S. M. AND WAINWRIGHT, P. C. (1990). The effect of sampling rate on the analysis of digital electromyograms from vertebrate muscle. *J. exp. Biol.* **154**, 557–565.

JOHNSON, T. P., SYME, D. A., JAYNE, B. C., LAUDER, G. V. AND BENNETT, A. F. (1994). Modeling red muscle power output during steady and unsteady swimming in largemouth bass. *Am. J. Physiol.* **267**, R481–R488.

JOHNSTON, I. A., FRANKLIN, I. A. AND JOHNSON, T. P. (1993). Recruitment patterns and contractile properties of fast muscle fibres isolated from rostral and caudal myotomes of the short-horned sculpin. *J. exp. Biol.* **185**, 251–265.

JOHNSTON, I. A. AND MOON, T. W. (1980). Endurance exercise training in the fast and slow muscles of a teleost fish (*Pollachius virens*). *J. comp. Physiol.* B **135**, 147–156.

LAUDER, G. V. AND LIEM, K. F. (1983). The evolution and interrelationships of the actinopterygian fishes. *Bull. Mus. comp. Zool.* **150**, 95–197.

LONG, J. H., JR, MCHENRY, M. J. AND BOETTICHER, N. C. (1994). Undulatory swimming: how traveling waves are produced and modulated in sunfish (*Lepomis gibbosus*). *J. exp. Biol.* **192**, 129–145.

MABEE, P. M. (1993). Phylogenetic interpretation of ontogenetic change: sorting out the actual and artefactual in an empirical case study of centrarchid fishes. *Zool. J. Linn. Soc. Lond.* **107**, 175–291.

ROME, L. C., FUNKE, R. P., ALEXANDER, R. M., LUTZ, G., ALDRIGE, H., SCOTT, F. AND FREADMAN, M. (1988). Why animals have different muscle fibre types. *Nature* **335**, 824–827.

ROME, L. C., LOUGHNA, P. T. AND GOLDSPINK, G. (1985). Temperature acclimation: improved sustained swimming performance in carp at low temperatures. *Science* **228**, 194–196.

ROME, L. C. AND SWANK, D. (1992). The influence of temperature on power output of scup red muscle during cyclical length changes. *J. exp. Biol.* **171**, 261–281.

ROME, L. C., SWANK, D. AND CORDA, D. (1993). How fish power swimming. *Science* **261**, 340–343.

SCOTT, W. B. AND CROSSMAN, E. J. (1973). *Freshwater Fishes of Canada*. Ottawa: Fisheries Research Board of Canada.

VAN LEEUWEN, J. L., LANKEET, M. J. M., AKSTER, H. A. AND OSSE, J. W. M. (1990). Function of red axial muscles of carp (*Cyprinus carpio*): recruitment and normalized power output during swimming in different modes. *J. Zool., Lond.* **220**, 123–145.

WALLÉN, P. AND WILLIAMS, T. L. (1984). Fictive locomotion in the lamprey spinal cord *in vitro* compared with swimming in the intact and spinal animal. *J. Physiol., Lond.* **347**, 225–239.

WARDLE, C. S. (1985). Swimming in marine fish. I*n Physiological Adaptations of Marine Animals, Symposium no. 39 of the Society of Experimental Biology* (ed. M. Laverak), pp. 521–540. Cambridge: Society of Experimental Biology.

WEBB, P. W. (1993). The effect of solid and porous channel walls on steady swimming of steelhead trout *Oncorhynchus mykiss*. *J. exp. Biol.* **178**, 97–108.

WEBB, P. W. (1994). The biology of fish swimming. In *Mechanics and Physiology of Animal Swimming* (ed. L. Maddock, Q. Bone and J. M. V. Rayner), pp. 45–62. Cambridge: Cambridge University Press.

WILLIAMS, T. L., GRILLNER, S., SMOLJANINOV, V. V., WALLÉN, P., KASHIN, S. AND ROSSIGNOL, S. (1989). Locomotion in lamprey and trout: the relative timing of activation and movement. *J. exp. Biol.* **143**, 559–566.